ELSEVIER

Chemical Engineering Journal 130 (2007) 67–74

Chemical Engineering Journal

www.elsevier.com/locate/cej

Aspects of liquor flow in a model chip digester measured using electrical resistance tomography

Frantisek Ruzinsky, Chad P.J. Bennington *

Department of Chemical and Biological Engineering, The University of British Columbia, 2360 East Mall, Vancouver BC V6T 1Z3, Canada

Abstract

Digesters for chemical pulping are pressurized reactors that create relative flow between process liquors and wood chips to delignify the wood and produce kraft pulp. As digester size has increased to accommodate higher production rates, operating problems related to liquor flow have increased. These have included accelerated corrosion, decreased countercurrent washing efficiency, problems with chip movement, and increased pulp non-uniformity. In this work, we used an 8-plane electrical resistance tomography (ERT) system to examine a number of important liquor flow issues in a 1/30 scale-model section of a chip digester: the effect of the particle to vessel size ratio on liquor flow uniformity, flow adjacent to the digester walls, and flow exiting the central downcomer.

Keywords: Electrical resistance tomography; Digesters; Liquor flow; Wood chips; Kraft pulp

1. Introduction

To produce kraft pulp, wood chips are reacted with aqueous process liquors (sodium hydroxide and sodium sulfide are the active chemicals) in large pressurized reaction vessels called digesters. The relative flow of liquor through the chip mass exposes all chips to a controlled chemical and thermal history, aimed at producing pulp having high strength and uniform residual lignin content. In the last decade, a number of modified cooking strategies have been introduced to improve pulp quality by optimizing chemical kinetics and thus reaction selectivity. These strategies increasingly rely on creation of uniform and well-defined liquor circulation zones through which the chip bed moves.

Liquor flow is unlikely to be uniform across a digester cross-section, particularly with existing digesters commonly operated well above original design capacity and new digesters fabricated for ever greater production rates. Both vessel scale-up and process modifications change liquor flows and are believed responsible for problems with accelerated corrosion [1–3], decreased pulp uniformity [4], decreased washing efficiency [5], decreased ease of chip movement [6] and build up of scales on vessel surfaces [7].

Very few measurements of chip or liquor flow have been made inside digesters. Hamilton [8] measured the movement of radioactively tagged tracer chips through a small digester and found plug flow with column compaction at the bottom of the digester. Changes in liquor flux through the cooking zone have been linked to changes in pulp properties, although debate concerning the magnitude of this effect exists [4,9]. The temperature of the digester shell has been used to infer liquor flow at the periphery of the wash zone, with significant improvements in uniformity made by controlling the wash dilution flow at the bottom of a digester [6]. However, flow uniformity at the centre of a digester cannot be measured.

Mathematical models of varying complexity have been developed to calculate liquor flow throughout the digester and assess its effects on pulp quality [10,11]. These models require assumptions of flow behavior (liquor and chip), selection of boundary conditions, and use of empirical models to describe physical phenomena affecting digester operation (*e.g.* chemical kinetics and interaction between the solid and liquid phases). Validation of the model predictions requires experimental data.

Electrical resistance tomography (ERT) has been used to measure liquor flow through a model-scale section of a digester for a number of industrially relevant configurations [12–14]. Tests show that to create a uniform zone within the vessel, the ratio of liquor flow in the radial direction (between the central downcomer and its corresponding screen section) to that in the axial direction (upflow or downflow) must be greater than or

* Corresponding author. Tel.: +1 604 822 8573; fax: +1 604 822 8563.
E-mail address: cpjb@chml.ubc.ca (C.P.J. Bennington).

1385-8947/$ – see front matter © 2007 Elsevier B.V. All rights reserved.
doi:10.1016/j.cej.2007.01.027

Nomenclature

A	vessel cross-sectional area (m^2)
d	representative particle diameter (m)
d_{32}	particle diameter $6V_p/S_p$ (m)
D	vessel diameter (m)
Q_A, Q_R	axial and radial volumetric flow rates (L/s)
r	radial distance (from the center) (m)
R	radius (m)
Re_p	particle Reynolds number
u	liquid velocity (m/s)
U	superficial liquid velocity (m/s)

Greek characters

ε	void fraction
μ	viscosity (Pa s)
ρ	density (kg/m^3)

Subscripts

c	centre
m	mid region ($r/R = 0.5$)
w	wall region
t	theoretical

equal to one. Zone uniformity increased as the radial liquor flux increased.

Here, we discuss issues related to liquor flow in the model digester. In past studies, industrial chips were used for the packed bed. This raises the issue of the effect of the ratio of column to particle diameter on liquid flow through the chip bed, in particular, on regions adjacent to the vessel walls. In addition, the effect of flow exiting the downcomer is critical for establishing radial uniformity in a zone and is unknown.

2. Experimental

A 1/30 scale-model ($D = 0.28$ m i.d.) of a digester zone, shown schematically in Fig. 1, was used in this study. Eight electrical resistance tomography (ERT) sensor planes (numbered consecutively from the bottom of the vessel) were spaced at 7.5 cm intervals along the digester axis with each plane consisting of 16 electrodes spaced equally around the vessel periphery. This allowed pseudo three-dimensional images of traced liquor flows to be made as a function of time. Data acquisition and image reconstruction were made using an ITS P2000 ERT system (Manchester, UK) and controlled by a PC.

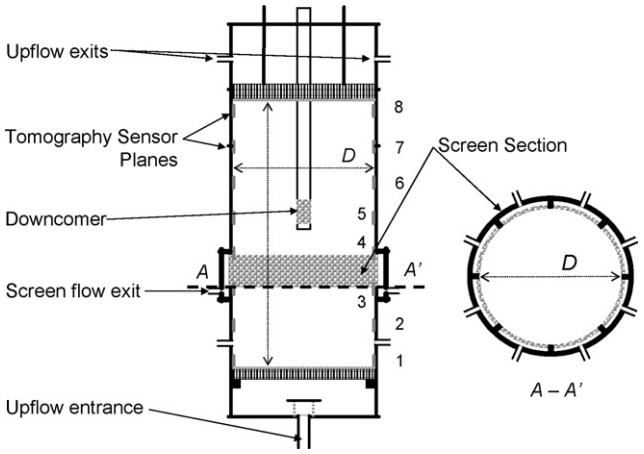

Fig. 1. Schematic diagram of model-scale digester. Imaging planes are numbered from the base of the vessel.

A fixed bed of solid particles (either wood chips or polyethylene disks) was added to the vessel. Two flow loops circulated liquid through the bed. The first pumped liquor axially through the vessel. The second circulated liquor radially through the downcomer-screen loop.

Two methods were used to trace liquor flow through the vessel. In the first method, the flow of interest was tagged using a brine solution having different conductivity than that of the background solution (which was typically 1.0 mS/cm). A step change in tracer concentration (by ±20%) was introduced to one of the flow circuits and imaged as a function of time. The second method involved introducing a tracer solution isokinetically through a tube (21.7 mm in diameter) positioned within the packed bed (Fig. 2). The tube diameter was chosen to be large enough to ensure detection by the ERT technique which has a spatial resolution of 5–10% of the vessel diameter (14–28 mm). During all tests the brine solution tracer was not returned to the storage tanks so that the concentration of the liquids entering the vessel remained constant.

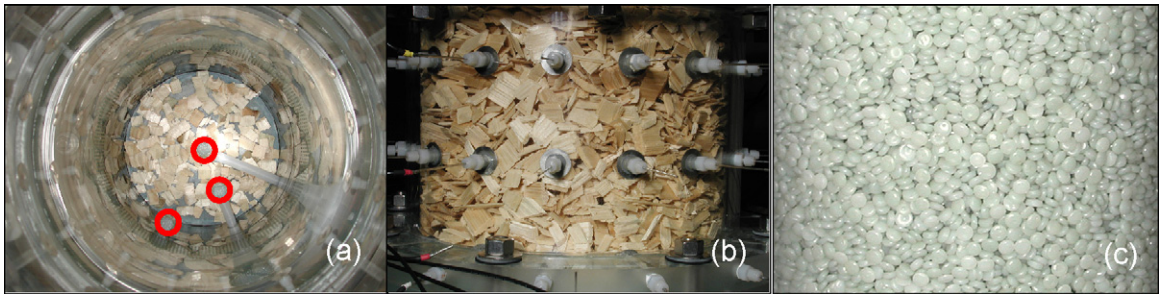

Fig. 2. Photographs of (a) the interior of the digester showing the locations of the injection tubes used for isokinetic tracer introduction. The feed tubes (highlighted in the picture) were positioned 13.5 cm above the digester base at r/R values of 0, 0.5 and 0.91; (b) side view of packed column of wood chips (for reference, the inside diameter of the vessel is 28 cm); and (c) side view of packed column of HDPE pellets (diameter of 4.4 mm).

Table 1
Particle Reynolds number for industrial and model systems

	Industrial digester		Model digester	
	Wood chips ($\varepsilon = 0.30$–0.50)	Wood chips ($\varepsilon = 0.53$)	Cooked chips[a] ($\varepsilon = 0.33$)	HDPE pellets ($\varepsilon = 0.35$)
Re_p (minimum)	23	14	22	4
Re_p (maximum)	96	56	89	29

Black liquor at 20% solids: 80 °C, $\rho = 1090\ kg/m^3$, $\mu = 0.92$ mPa s
180 °C, $\rho = 1040\ kg/m^3$, $\mu = 0.39$ mPa s
Brine solution (1 mS/cm): 20 °C, $\rho = 999\ kg/m^3$, $\mu = 1.002$ mPa s

[a] Black Spruce accept chips cooked to kappa 44.

3. Results and discussion

3.1. Ratio of column to particle diameter

In our previous work, the liquid flow through the packed beds of wood chips has been modelled by keeping the particle Reynolds number, $Re_p = d_{32}u\rho/\mu$ (calculated assuming uniform axial flow), identical to the industrial case as shown in Table 1. Here, d_{32} is the volume–surface mean particle diameter, u the liquor velocity ($Q/A\varepsilon$), and ρ and μ are the liquid density and viscosity. In the industrial case, the parallelepiped wood chips have typical dimensions of 25 mm × 20 mm × 4 mm, the bed void fraction varies as the cook progresses but is typically in the range of $\varepsilon = 0.50$–0.30, and the relative liquor superficial velocity can reach 9 mm/s [10]. For our laboratory investigations slightly smaller chips (17.5 ± 2.2 mm × 15.5 ± 6.3 mm × 3.3 ± 1.1 mm) were used with the void fraction and liquid velocity matched to the industrial case. However, as industrial digesters can exceed nine metres in diameter, the ratio between the column and chip diameters is significantly different between the industrial and laboratory scales (Table 2). This ratio characterizes the size of the wall-affected zone which extends from the wall into the chip bed.

The packed column can be divided into three radial zones: a wall region, a transition region and a bulk region. Cohen and Metzner [15] examined packed beds of spherical particles and found that the wall region (having increased particle voidage and influenced by the vessel wall) extended one particle diameter from the periphery; the transition region (in which significant voidage oscillations occurred) extended a distance of six particle diameters from the wall; and the bulk region (where the bed voidage was uniform) filled the remainder of the bed cross-section. For beds where the column to particle diameter ratio was less than 30, the transition region occupied the largest fraction of the column cross section. If we apply Cohen and Metzner's criterion to our laboratory experiments with packed chips, the wall and transition regions occupy 24% of the cross-sectional area.

Table 2
Column to particle diameter ratio

	Industrial digester ($D = 5$–8 m)	Model digester ($D = 0.28$ m)	
	Wood chips	Wood chips	HDPE pellets
d[a] (mm)	25.2	18.2 ± 4.0	4.44 ± 0.19
d_{32} (mm)	8.82	6.81 ± 1.65	3.08 ± 0.21
D/d	198–317	15	63
D/d_{32}	567–907	41	91

[a] Length dimension of chip, diameter of HDPE disk.

When disk shaped particles of high-density polyethylene (HDPE) having a diameter of 4.44 ± 0.19 mm and a thickness of 1.91 ± 0.19 mm were used in the laboratory digester, the column to particle ratio was increased and the wall and transition affected regions reduced to 11% of the column cross-section. However, the particle Reynolds number was reduced and the area occupied by the wall and transitional regions was still much larger than would be found in an industrial digester. A bed of these HDPE disks has a void ratio of $\varepsilon = 0.346 \pm 0.006$.

Fig. 3 gives tomographic reconstructions made along the centerline of the digester axis for three scenarios of interest in a continuous digester wash zone with HDPE disks used as the model particles. In these tests, a split between liquor flows was made to give ratios of axial (upflow in all cases), Q_A, to radial flow, Q_R, of 0.5, 1.0 and 2.0. These are the same ratios used by Vlaev and Bennington [12,13] in their work with wood chips. In our tests, digester flows were stabilized with liquor having a conductivity of 1.0 mS/cm. A step change was then introduced with the fluid entering the downcomer changed from 1.0 to 0.78 mS/cm. The upflowing liquor was maintained at 1.0 mS/cm. The change in flow patterns was tracked as a function of time with the images shown in Fig. 3 made after steady-state was attained. In this, and all succeeding figures, the mid-plane images through the digester axis are oriented left to right, while the individual plane images are oriented L–R with the front projection at the bottom of each circle.

The tomographic images confirm the results reported previously for both cooked and uncooked chips [12,13]. When radial flow exceeded upflow ($Q_A/Q_R = 0.5$) all the upflowing fluid was directed to the screens creating distinct zonal regions between the upper and lower digester. As the flow split was changed to 1:1, a more pronounced "V" profile was found below the screens than observed previously for the wood chips. This was likely due to differences in flow-induced diffusion in the radial direction caused by the solid phase (as the diameter of the HDPE pellets is significantly smaller than that of the wood chips and they both orient in the horizontal direction as they are packed). The tomograms also clearly show the presence of higher conductivity tracer above the screen level indicating some bypassing of the upflowing liquid. When upflow was increased so that

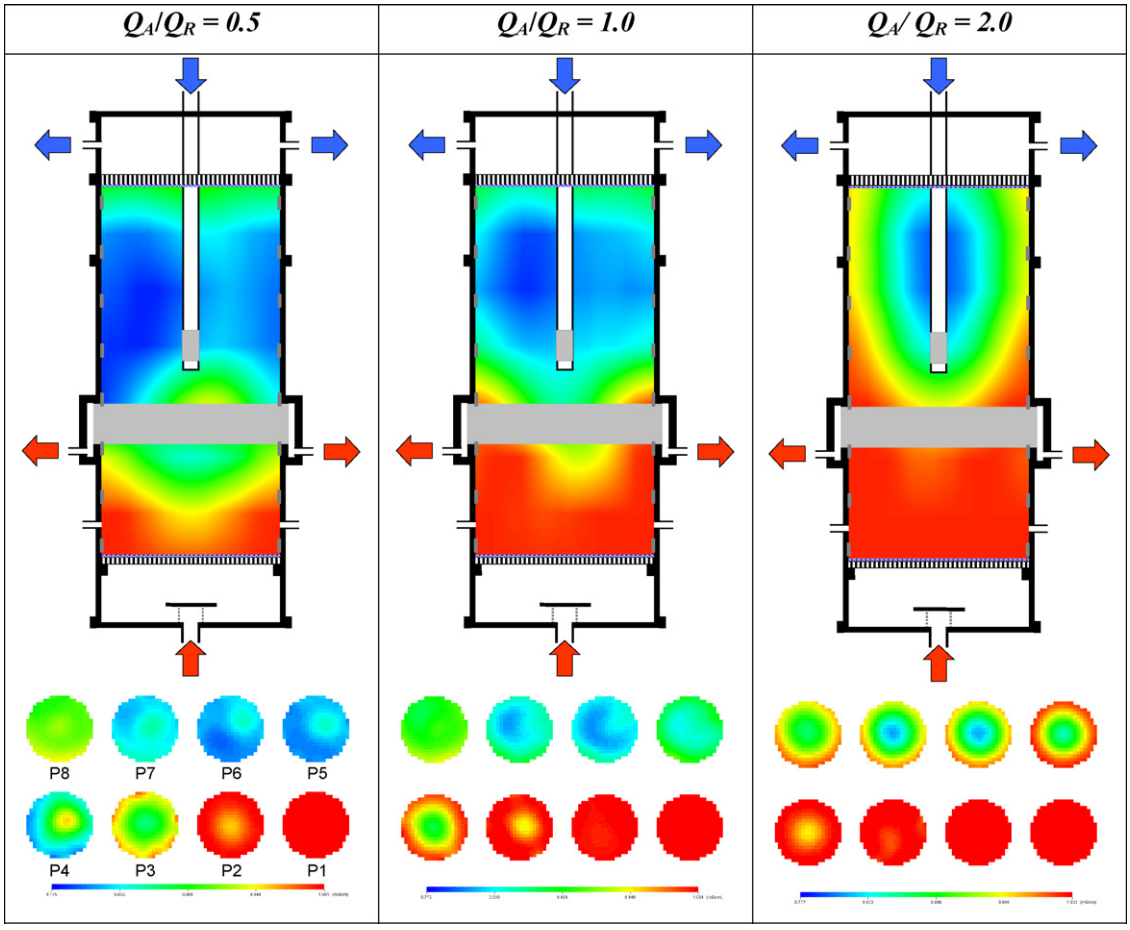

Fig. 3. Tomographic images of liquid concentration through a packed bed of HDPE pellets at the steady-state. A step reduction in liquor conductivity was made in the flow exiting the downcomer. Images give the concentration distribution at steady-state for flow ratios of Q_A/Q_R of 0.5, 1.0 and 2.0. A total liquid flux of 75 mL/s was used for Q_A/Q_R of 0.5 and 2.0 and of 50 mL/s at Q_A/Q_R equal to 1.0. The planes are numbered from the bottom. In this, and the other tomographic diagrams, low conductivity regions are colored blue and high conductivity regions are colored red.

$Q_A/Q_R = 2.0$, the upflow liquor passed the screen zone forming an annular ring that continued upwards in the vessel. A thin zone of more concentrated brine moved adjacent to the walls through the entire upper vessel creating a radial gradient of concentration towards the central downcomer. In the case shown in Fig. 3, the film thickness was different between the front and back of the vessel, likely caused by slightly different flow rates through the segmented screen section.

Mass balances made on the salt entering and leaving the digester confirm the analysis presented above. Fig. 4 gives the conductivity of tracer leaving the screen and upflow exits as a function of time following the step reduction in tracer conductivity entering the downcomer. For $Q_A/Q_R = 0.5$, the predicted liquor conductivities exiting the screen and overflow sections are 0.882 and 0.766 mS/cm, respectively, assuming that the streams remain completely segregated. The measured conductivities of 0.882 and 0.768 mS/cm confirm this. For a flow ratio of 2.0, the mass balance only closed to ±2.5% and it was not possible to compute exit conductivities with sufficient accuracy to confirm if complete segregation existed when axial flow exceeded the downcomer-screen circulation flow. For the case where $Q_A/Q_R = 1.0$, perfect segregation of the flows would be

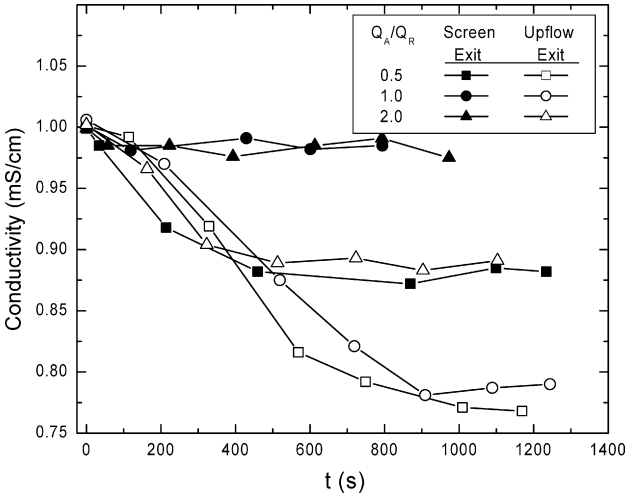

Fig. 4. Conductivity versus time for brine solutions exiting the screen and overflow sections of the laboratory digester following a step change in brine concentration introduced into the downcomer flow. Identical test conditions as presented in Fig. 3. The initial (background) conductivity ranged from 0.997 to 1.006 mS/cm with the conductivity of the downcomer flow changed in a step manner to 0.766–0.777 mS/cm.

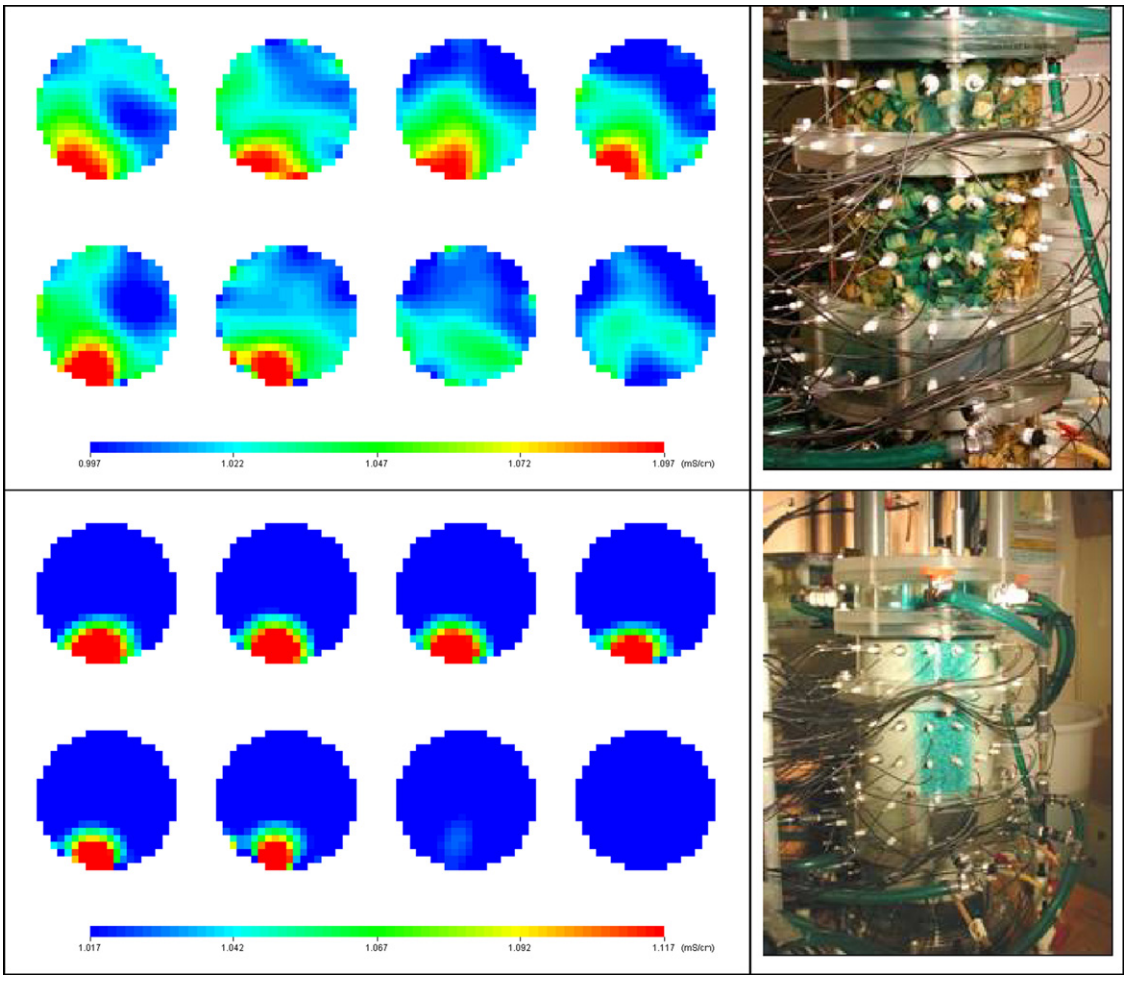

Fig. 5. Tomographic images and photographs showing steady-state flow of a plume of conductive tracer injected isokinetically into an upflow of $Q = 200$ mL/s through a packed bed of (a) wood chips ($\varepsilon = 0.53$) and (b) HDPE pellets ($\varepsilon = 0.35$) near the wall ($r/R = 0.91$).

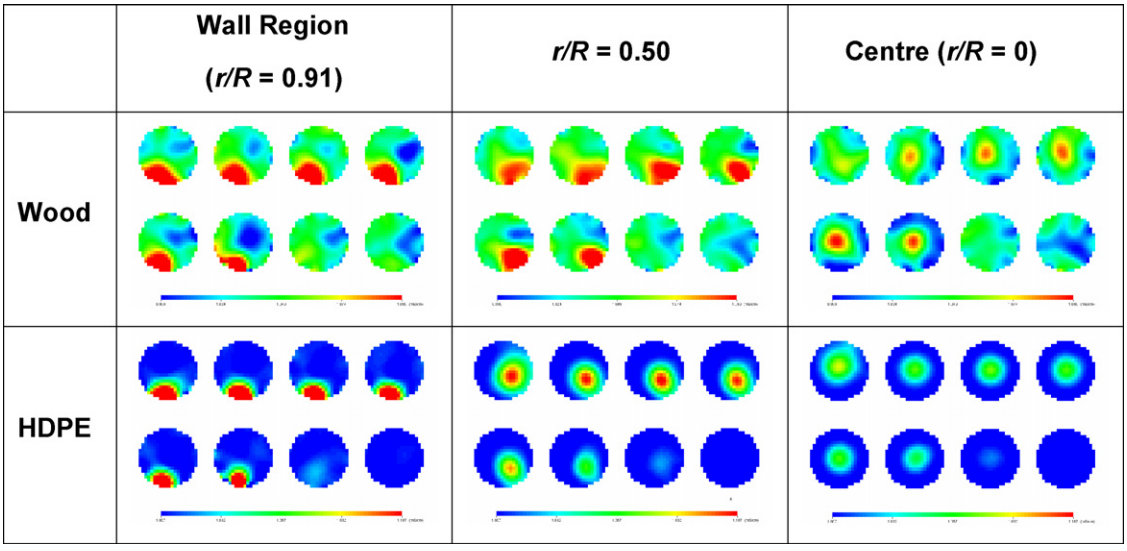

Fig. 6. Tomographic images after establishment of steady flow showing the plume of more conductive tracer injected isokinetically into a bed of (a) wood chips ($\varepsilon = 0.53$) and (b) HDPE pellets ($\varepsilon = 0.35$) at a calculated upflow velocity of 6.1 mm/s for three locations within the bed.

Table 3
Local velocity in packed wood chip bed

Q (mL/s)	Liquid rise velocity (mm/s)				u_w/u_c
	u_t	u_w	u_m	u_c	
50	1.5	2.4 ± 0.04	1.5 ± 0.06	1.1 ± 0.09	2.1
100	3.1	3.5 ± 0.04	2.5 ± 0.24	1.9 ± 0.13	1.9
200	6.1	7.5 ± 0.44	4.4 ± 1.03	3.9 ± 0.48	1.9

expected to give a concentration of 1.006 mS/cm at the screens and 0.772 mS/cm at the overflow. The values measured, 0.985 and 0.772 mS/cm, indicate that some mixing between these streams must have occurred—about 2%. This helps confirm the tomographic data which detected a region of more concentrated liquor above the screen section.

3.2. Localized liquor axial flow

Visual and tomographic comparison of flow adjacent to the wall in the packed bed of wood chips and HDPE pellets are given in Fig. 5. Here a green dye was added isokinetically to a 5 mS/cm brine solution injected at the wall region of the vessel ($r/R = 0.91$) for a volumetric flow rate of 200 mL/s (no downcomer-screen circulation flow was used and the downcomer was removed from the bed). The tomographic images match the dye pattern observed at the wall very well. In the chip bed, the tracer spreads significantly, while the tracer plume in the HDPE pellets does not spread as extensively.

In Fig. 6, tomographic images are shown for isokinetic tracer injection in upflow through chips and HDPE pellets at the wall, a location mid-way between the wall and the centre of the vessel, and the centre of the vessel for an upflow velocity of $u_t = 6.1$ mm/s. We note again that the flow through the chip bed significantly spreads in the radial direction and looses its well-defined shape as it rises through the bed. The flow through the HDPE pellets, in contrast, retains a more distinct shape.

Temporal images from these experiments were used to measure the local rise velocity at the three radial positions in the digester. The data are presented in Tables 3 and 4, which give the theoretical rise velocity, u_t (calculated assuming uniform flow across the vessel cross-section) and the velocity measured at each location (wall region, u_w; mid-point at $r/R = 0.50$, u_m, and at the centre of the vessel, u_c). For the HDPE pellets the rise velocity was measured using two procedures. The first entry in Table 4 gives the velocity measured using isokinetic injection of a 5.0 mS/cm tracer into a 1.0 mS/cm background solution. The second entry used isokinetic injection of distilled water into a 1.0 mS/cm background solution. Only the former technique was used for the wood chips.

Table 4
Local velocity in packed bed of HDPE pellets

Q (mL/s)	Liquid rise velocity (mm/s)				u_w/u_c
	u_t	u_w	u_m	u_c	
50	2.3	2.3/2.6	3.1/2.6	2.9/2.1	0.8/1.2
66	3.1	2.6/2.9	3.2/3.0	3.3/2.8	0.8/1.0
100	4.6	4.3/4.4	4.9/4.6	5.2/4.3	0.8/1.0
132	6.1	5.3/6.2	6.2/4.9	6.2/5.0	0.8/1.3
200	9.3	8.8/9.2	10.0/7.9	9.1/9.8	1.0/0.9

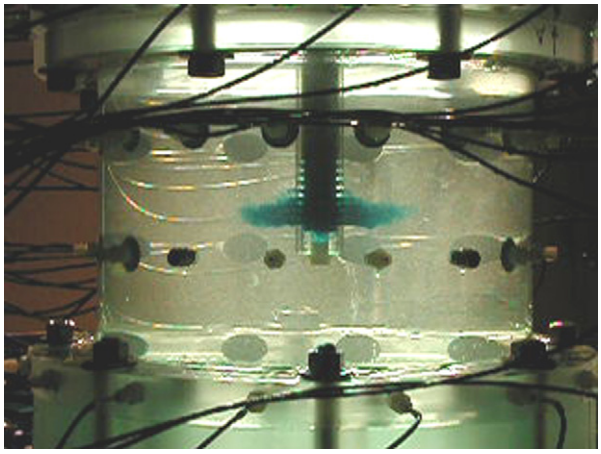

Fig. 7. Photograph of a pulse of tracer dye exiting the central downcomer. $Q = 126$ mL/s. Flow is seen exiting only the bottom half of the downcomer open area.

The reproducibility of the velocity determinations ranged from 1 to 23% (COV). The accuracy of the velocity measurements was limited by the ability to detect the tracer plume as it crossed a given sensor plane and the time interval between sampling at each plane. This allowed us to estimate the COV of a velocity determination as being from 10 to 15%, in the range measured.

The ratio of flow velocities at the wall and centre of the vessel are given in the last column of Tables 3 and 4. For the wood chips, the measured flow at the wall and mid-point locations (within the wall and transition zones defined by Cohen and Metzner [15]) was significantly greater than the theoretical velocity calculated assuming uniform flow through the vessel. The flow at the wall was close to twice the value measured in the centre of the column. This confirms greater flow at the wall and wall affected regions as reported in the literature [15]. For the HDPE pellets, the flow was much more uniform across the column cross-section and the flow ratio u_w/u_c was close to 1.0. For the HDPE pellets, the wall-affected region was much smaller and the size and proximity of the feed tube to the wall did not permit any difference in velocity to be detected.

3.3. Liquor flow in the vicinity of the downcomer

Liquor exiting the downcomer is meant to do so uniformly in both the radial and axial directions. Our tomography studies indicate that radial uniformity can be achieved when the radial flow from the downcomer and screen are uniform. However, the role of axial uniformity along the downcomer is not known (the exit nozzles are spaced over a vertical distance of 4 cm). The resolution of the tomograms in the axial direction is not fine enough to measure this. However, visual observations made of dyed tracer exiting the downcomer (into stationary water) show that the radial discharge along the downcomer axis is far from uniform (Fig. 7). For the test conditions depicted here, the

liquid exits primarily through the bottom four nozzles of the downcomer, with significantly reduced flow through the upper four nozzles. This may have a profound impact on the liquid flow set up in the vessel.

Fig. 8 gives two-dimensional flow velocities for selected locations measured along the centre-line of the vessel axis for $Q_A/Q_R = 0.5$ and 1.0 with $Q_A = 100$ mL/s using the HDPE pellets ($\varepsilon = 0.35$). Velocities were measured by following the moving front of a tracer stream (at the point corresponding to a signal ±27% different than the background value) in the axial and radial planes as a function of time. Tracer injection was done in a number of points: into the downcomer for velocity measurements above the screen level; into the axial flow entering the vessel for velocity measurements below the screen level; and using isokinetic injection for velocity measurement at the screen level. The accuracy with which the velocity could be measured varied from 15 to 36% due to the temporal and spatial resolution of the front. Velocities were best measured in the axial direction as the front moved between the planes and in the radial location on a sensor plane axis. The dotted lines in the figure correspond to flow streamlines observed from tracer tests.

Below the screen section flow is upward. Velocity is greatest along the wall of the digester, due in part to the wall effects discussed earlier, but primarily attributed to flow exiting the downcomer which inhibits upward flow from below. At the screen level, flow exits radially through the screens, with the highest velocities found immediately adjacent to them. A stagnation point exists immediately below the downcomer at the centre of the vessel at the mid-screen level. Above the screen zone, flow moves rapidly upwards, particularly immediately adjacent to the downcomer which is attributed to the wall-affected region. As downcomer flow is increased (from 100 to 200 mL/s) velocities in the upper region and screen section of the vessel increase.

4. Summary and conclusions

Electrical resistance tomography was used for imaging the flow characteristics in a column configured to operate as the wash section of a continuous digester. When the packed bed is modeled using HDPE pellets, the ratio of vessel to particle diameter is closer to that of the industrial situation. This permits better resolution of the liquid flow regions within the vessel, although the particle Reynolds number now deviates from the industrial situation. With the HDPE particles, system noise was also lower which permitted better image reconstruction, likely due to the material properties of the particles.

Tests made with wood chips showed that liquid flow adjacent to the vessel wall was significantly greater than at the centre of the vessel. This difference was not as extreme for the HDPE disks for which the wall-affected zone is much smaller and below the spatial resolution of the ERT system.

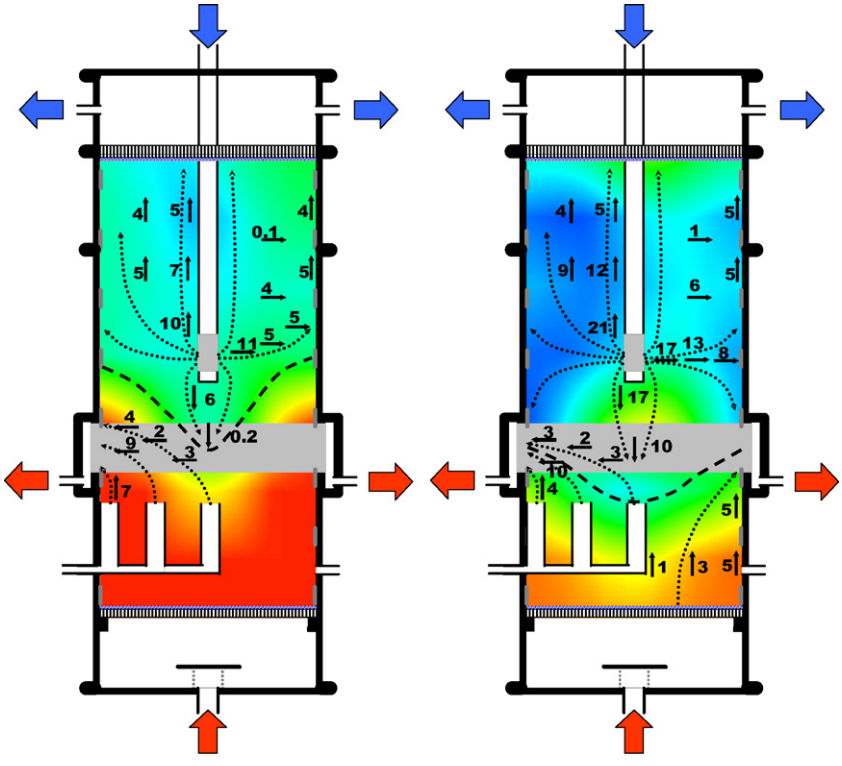

Fig. 8. Tomographic images showing steady-state liquid velocities (mm/s) measured at selected locations in the vessel for $Q_A/Q_R = 0.5$ and 1.0 with $Q_A = 100$ mL/s. Packed bed of HDPE disks ($\varepsilon = 0.35$). The dotted and dashed lines show flow streamlines estimated from steady-state tomograms.

The axial resolution of the ERT system in its present configuration is insufficient to image axial uniformity of flow exiting the downcomer. ERT reconstructions of tracer added isokinetically below the downcomer showed that all tracer exited the downcomer when Q_R was twice Q_A. For a 1:1 flow ratio, some tracer was detected above the screen level.

Local velocities were measured using temporal data. The effect of the downcomer flow was shown to suppress upflow immediately below the downcomer, contributing to a stagnant zone at the screen level in the centre of the vessel. Flow velocity adjacent to the downcomer was huge—in part likely due to the wall effect of the downcomer which increases local voidage in its vicinity.

References

[1] J. Wale, S. Lahti, G. Sund, Survey of recent years corrosion damage development in the Swedish pulp and paper industry, in: Proceedings on 8th International Symposium on Corrosion in the Pulp and Paper Industry, SPCI, Stockholm, Sweden, May 16–19, 1995, pp. 233–239.

[2] L. Kiessling, A study of the influence of modified continuous cooking processes on the corrosion of continuous digester shells, in: Proceedings on 8th International Symposium on Corrosion in the Pulp and Paper Industry, SPCI, Stockholm, Sweden, May 16–19, 1995, pp. 12–19.

[3] A. Wensley, Corrosion and protection of kraft digesters, Tappi J. 79 (10) (1996) 153–160.

[4] A.J. Horng, D.M. Mackie, J. Tichy, Factors affecting pulp quality from continuous digesters, Tappi J. 70 (12) (1987) 75–79.

[5] N. Lorincz, B. Marcoccia, Downflow cooking trials at the DMI, Peace River Mill, in: Proceedings on Pacific Coast and West Branches Conference, PAPTAC, Whistler, BC, Canada, May 16–19, 2001.

[6] G. Pageau, B. Marcoccia, New filtrate addition system results in improved digester performance, in: Proceedings on Pacific Coast and West Branches Conference, PAPTAC, Whistler, BC, Canada, May 16–19, 2001.

[7] W. Reyngoud, I.J. Whyte, P. Stoove, Restoring the circulation in a continuous digester, Appita J. 47 (2) (1994) 134–136.

[8] P.O. Tikka, J.M. Macleod, K.K. Kovasion, Chemical and physical performance of kraft cooking: the impact of process alternatives, Tappi J. 74 (1) (1991) 137–143.

[9] R.P. Hamilton, Measurement of Kamyr continuous kraft digester cooking cycle using radioactive tracers, Tappi 44 (9) (1961) 647–655.

[10] E.J. Harkonen, A mathematical model for two-phase flow in a continuous digester, Tappi J. 60 (12) (1987) 122–126.

[11] P. He, M. Salcudean, I. Gartshore, E. Bibeau, Modeling of kraft two-phase digester pulping processes, in: TAPPI Engineering Process and Product Quality Conference, TAPPI, Anaheim, CA, USA, September 12–16, 1999, pp. 1407–1418.

[12] D. Vlaev, C.P.J. Bennington, Flow of Liquor through Wood Chips in a Model Digester, AIChE Annual Meeting, San Francisco, CA, November 16–21, 2003.

[13] D. Vlaev, C.P.J. Bennington, Flow uniformity in a model digester measured with electrical resistance tomography, in: 3rd International Congress on Industrial Process Tomography, Banff, AB, Canada, September, 2003, pp. 821–827.

[14] D. Vlaev, C.P.J. Bennington, Using electrical resistance tomography to image liquor flow in a model digester, J. Pulp Paper Sci. 30 (1) (2004) 15–21.

[15] Y. Cohen, A.B. Metzner, Wall effects in laminar flow of fluids through packed beds, AIChE J. 27 (1981) 705–715.